CHEMISTRY
A EUROPEAN JOURNAL

DOI: 10.1002/chem.201102300

Tridentate N-Donor Palladium(II) Complexes as Efficient Coordinating Quadruplex DNA Binders

Eric Largy,[a] Florian Hamon,[a] Frédéric Rosu,[b] Valérie Gabelica,[b] Edwin De Pauw,[b] Aurore Guédin,[c] Jean-Louis Mergny,[c] and Marie-Paule Teulade-Fichou*[a]

Abstract: Fifteen complexes of palladium, platinum, and copper, featuring five different N-donor tridentate (terpyridine-like) ligands, were prepared with the aim of testing their G-quadruplex–DNA binding properties. The fluorescence resonance energy transfer melting assay indicated a striking positive effect of palladium on G-quadruplex DNA stabilization compared with platinum and copper, as well as an influence of the structure of the organic ligand. Putative binding modes (noncoordinative π stacking and base coordination) of palladium and platinum complexes were investigated by ESI-MS and UV/Vis spectroscopy experiments, which all revealed a greater ability of palladium complexes to coordinate DNA bases. In contrast, platinum compounds tend to predominantly bind to quadruplex DNA in their aqua form by noncoordinative interactions. Remarkably, complexes of [Pd(ttpy)] and [Pd(tMebip)] (ttpy = tolylterpyridine, tMebip = 2,2′-(4-*p*-tolylpyridine-2,6-diyl)bis(1-methyl-1*H*-benzo[d]imidazole)) coordinate efficiently G-quadruplex structures at room temperature in less than 1 h, and are more efficient than their platinum counterparts for inhibiting the growth of cancer cells. Altogether, these results demonstrate that both the affinity for G-quadruplex DNA and the binding mode of metal complexes can be modulated by modifying either the metal or the organic ligand.

Keywords: DNA · FRET · G-quadruplexes · mass spectrometry · transition metals

Introduction

Guanine (G)-rich DNA and RNA sequences have the ability to fold into four-stranded helicoidal structures called G-quadruplexes (abbreviated to G4s). A large number of sequences identified by bioinformatics studies[1] may form various quadruplex structures, which share the G-quartet as a common monomeric motif, but differ in the loop arrangements.[2] A G-quartet is the association of four guanines by Hoogsteen hydrogen bonds in a coplanar fashion. This motif self-stacks through π–π aromatic forces and by sandwiching alkaline cations (Na^+, K^+), which participate greatly in the stability of the quadruplex structure. It is now widely assumed that G4 DNA may interfere with various biological events related to the transfer and maintenance of genetic information (replication, transcription, telomeric functions, translation, etc.), and thereby, could be involved in the regulation of gene expression.[3] The synthesis of small molecules capable of targeting G4 DNA is a rapidly expanding field: these compounds could act pharmacologically through sequence/structure specificity and allow better understanding of the biological role(s) of quadruplexes.[4] Small molecules usually bind to G4 DNA through π-stacking interactions with external G-quartets, but some also interact with the loops[5] and grooves.[6]

Since the discovery more than 40 years ago that cisplatin derivatives could act as antitumor agents,[7] an extensive number of metal complexes aimed at binding DNA have been synthesized. Predictably, metal complexes have also emerged in the G4 DNA field and display various binding modes (π stacking, metalation of bases, cleavage).[8] The advantages of using metal complexes are numerous. Different metal cations adopt diverse geometries for a given ligand, while introducing positive charges. Moreover, the metal can withdraw electrons from the ligand, thus making it more suitable for π stacking with electron-donor bases, such as guanines. Terpyridine (tpy) derivatives with a tolyl moiety (ttpy) or an extended aromatic surface (dibenzoterpy (BisQ); Scheme 1) have been successfully used to prepare transition-metal complexes (Pt^{2+}, Cu^{2+}) that have shown high binding affinity for the human telomeric G4.[9] In particular, [Pt(ttpy)] selectively platinates adenine bases located in the loops of this quadruplex structure.[10] Square-planar platinum(II) complexes, with two exchangeable ligands, such as cisplatin,[11] or one, such as tpy complexes,[12] can coordi-

[a] E. Largy, Dr. F. Hamon, Dr. M.-P. Teulade-Fichou
UMR176 CNRS, Institut Curie, Centre de Recherche,
Centre Universitaire, 91405 Orsay (France)
Fax: (+33) 169-07-53-81
E-mail: marie-paule.teulade-fichou@curie.fr

[b] Dr. F. Rosu, Dr. V. Gabelica, Prof. E. De Pauw
Mass Spectrometry Laboratory, Chemistry Institute B6C
Université de Liège, 4000 Liège (Belgium)

[c] A. Guédin, Dr. J.-L. Mergny
Université de Bordeaux, Inserm U869, IECB,
ARNA laboratory. 2 Rue Robert Escarpit, 33607 Pessac (France)

Supporting information for this article is available on the WWW under http://dx.doi.org/10.1002/chem.201102300.

WILEY ONLINE LIBRARY
© 2011 Wiley-VCH Verlag GmbH & Co. KGaA, Weinheim

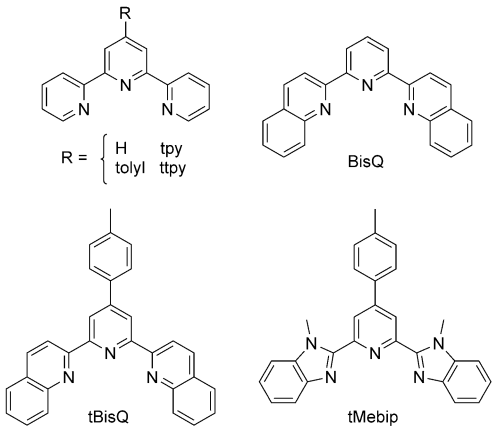

Scheme 1. Structures of tridentate N-donor ligand described herein.

nate to DNA bases (with a strong preference for guanine N7) after a hydrolysis step (aquation), which is the rate-limiting step and highly dependent on the chelating ability of the ligand coordinated to the metal.[13] Palladium(II) and platinum(II) are soft Lewis acids and share the same square-planar geometry.[14] They display similar characteristics when coordinated to N-donor polydentate ligands, but interestingly, the key difference rests on the ligand-exchange kinetics, in particular, during the aquation reaction. Hydrolysis rates are much faster for palladium than for platinum complexes (10^5 times faster according to instrumental methods,[15] and 10^6 times estimated by ab initio studies[16]). This results in kinetic instability of Pd–DNA complexes relative to their Pt counterparts, which has limited the use of Pd derivatives for DNA targeting and for biomedical applications. Nevertheless, because this property can be modulated by the nature of the heterocyclic ligand surrounding the metal, interest is now gradually shifting towards palladium and other transition-metal complexes for biomedical applications.[17]

Based on the reasons outlined above, we speculated that the introduction of palladium to our metal tpy G4 binders could modulate both noncoordinative binding and the coordination capability of quadruplex structures. Therefore, we launched a program aimed at modulating both the ligand surface and the coordinating metallic cation. It is worth noting that palladium complexes devoted to quadruplex DNA recognition have already been synthesized by Vilar et al. but the series investigated did not display strong binding affinities for the targeted DNA.[18]

Bis(*N*-methylbenzimidazolyl)pyridine (Mebip) is a tridentate nitrogen ligand often used in inorganic chemistry as an analogue of tpy, but compared with the latter, it is a moderate σ donor and also a π acceptor.[19] The larger aromatic surface, relative to tpy, seems to be more suited to π overlap with a G-quartet.[4b] For instance, the benzimidazole motif is a purine mimic that may stack efficiently on DNA bases[20] and has already been used to construct quadruplex-DNA ligands.[21] In addition, the bis(benzimidazole)pyridine core was recently shown to lead to efficient quadruplex ligands,[21a] including luminescent platinum complexes.[22] In the case of the tpy complexes, a tolyl group in the *para* position of the central pyridine ring dramatically increased the quadruplex binding affinity.

We therefore envisaged the preparation of the tolyl derivative of the Mebip ligand (tMebip; 2,2′-(4-*p*-tolylpyridine-2,6-diyl)bis(1-methyl-1*H*-benzo[d]imidazole)), which combined the structural features of ttpy and benzimidazole scaffolds, to prepare a metal complex with improved G4-recognition properties. Similarly, the tolyl moiety was introduced into the dibenzoterpyridine (BisQ) scaffold used in previous studies,[10] thereby affording a second ligand (tBisQ) featuring a tolylpyridine core and an extended aromatic surface. The five ligands derived from the tpy model (Scheme 1) were combined with the three metallic cations (Pd^{2+}, Cu^{2+}, Pt^{2+}). Binding affinities, binding modes, and binding kinetics of the five metal complex families for G4 DNA were investigated by fluorescence resonance energy transfer (FRET) melting,[23] electrospray mass spectrometry experiments,[24] and time-dependent UV/Vis absorbance measurements.

Results and Discussion

Synthesis of complexes: tMebip was prepared in three steps from chelidamic acid, with an overall yield of 45% (Scheme 2). Formation of benzimidazoles was achieved by thermal cyclization of chelidamic acid and *N*-methyl-1,2-phenylenediamine in the presence of polyphosphoric acid, which was used as a solvent.[25] Position 4 of the pyridine was then brominated by phosphorus oxybromide,[26] allowing

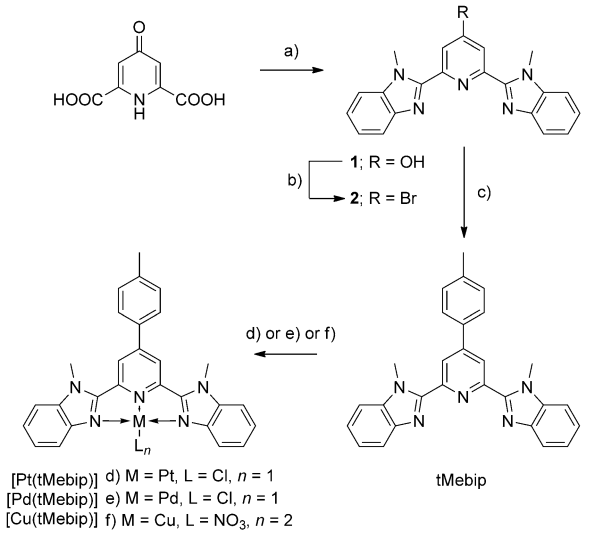

Scheme 2. Synthesis of tMebip complexes. Reagents and conditions: a) *N*-methylbenzene-1,2-diamine, polyphosphoric acid (PPA), 215°C, 17 h; b) $POBr_3$, 140°C, 17 h; c) *p*-tolylboronic acid, $[Pd(PPh_3)_4]$, K_2CO_3, THF/water, reflux, 24 h; 45% yield over three steps. d) K_2PtCl_4, nitromethane, reflux, 24 h, 15% yield; e) $[Pd(cod)Cl_2]$ (cod = 1,5-cyclooctadiene), DMF, 50°C, 24 h, 48% yield; f) $Cu(NO_3)_2$, CH_2Cl_2, acetonitrile, 4°C, 48 h, 42% yield.

 © 2011 Wiley-VCH Verlag GmbH & Co. KGaA, Weinheim

the introduction of the tolyl group through a Suzuki coupling.[27] The final product was easily obtained because it precipitated at room temperature in the THF/water mixture used as the solvent. This synthesis can be performed on the gram scale and requires few purification steps.

BisQ was prepared by following procedure described in the literature[10] based on a double Friedländer condensation between two equivalents of 2-aminobenzaldehyde and 2,6-acetylpyridine (Scheme 3). 2-Aminobenzaldehyde is not

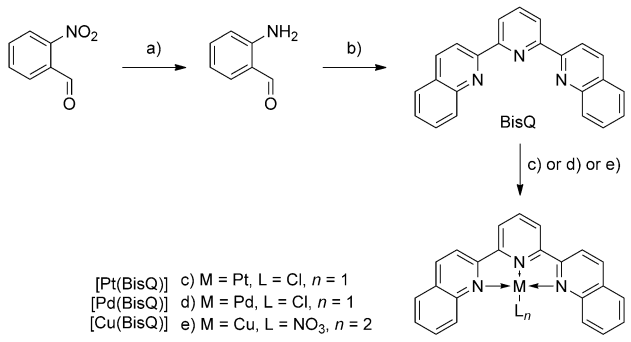

Scheme 3. Synthesis of BisQ complexes. Reagents and conditions: a) iron powder, 0.1 N HCl (aq), 95 °C, 30 min; b) 2,6-diacetylpyridine, potassium hydroxide, 95 °C, 1 h; 75 % yield over two steps in a one-pot procedure; c) K_2PtCl_4, nitromethane, reflux, 24 h, 21 % yield; d) [Pd(cod)Cl_2], DMF, 50 °C, 24 h, 84 % yield; e) $Cu(NO_3)_2$, CH_2Cl_2, acetonitrile, 4 °C, 48 h, 52 % yield.

stable,[28] and thus, it was generated in situ by reduction of 2-nitrobenzaldehyde.[29] An overall yield of 75 % was obtained for the two-step, one-pot process.

The synthesis of tBisQ was less straightforward and was achieved in 4 steps (Scheme 4) with an overall yield of 27 %.

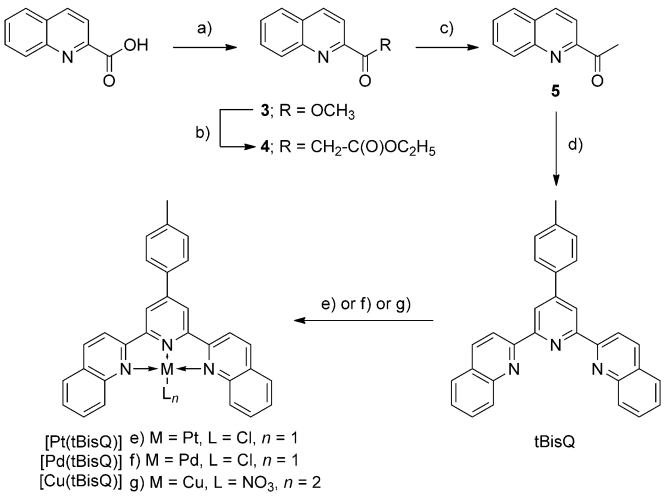

Scheme 4. Synthesis of tBisQ complexes. Reagents and conditions: a) sulfuric acid, MeOH, reflux, 16 h, 89 % yield; b) *t*BuOK, ethyl acetate, RT, 15 min, 79 % yield; c) HCl, dioxane, 100 °C, 16 h, 70 % yield; d) 4-methylbenzaldehyde, KOH, aqueous ammonia, EtOH, 100 °C, sealed tube, 24 h, 54 % yield; e) $K_2[PtCl_4]$, nitromethane, reflux, 24 h, 94 % yield; f) [Pd(cod)Cl_2], DMF, 50 °C, 24 h, 40 % yield; g) $Cu(NO_3)_2$, CH_2Cl_2, acetonitrile, 65 %.

The key intermediate, 2-acetylquinoline (**5**), was obtained by esterification of quinaldic acid, followed by Claisen condensation, and then a saponification/decarboxylation step. The ligand was finally obtained in 54 % yield by a double Kröhnke reaction, using a double condensation with aqueous ammonia on 2-acetylquinoline, ammonium acetate, and 4-methylbenzaldehyde under harsh conditions in a sealed tube at 100 °C for 24 h.[30]

Palladium, platinum, and copper complexes of BisQ, tBisQ, and tMebip were prepared by adapting procedures described in the literature.[9,31] These complexes were obtained in lower yields than those with tpy and ttpy, presumably because of their larger aromatic surface, which delocalizes the nitrogen lone-pair electrons.

FRET melting assay: The binding performances of the free ligands and their corresponding complexes were first evaluated by FRET melting assays. This well-known assay is based on monitoring the stability induced by binding of a ligand to a fluorescently labeled quadruplex structure, such as the human telomeric sequence F21T (*FAM*-$G_3(T_2AG_3)_3$-*Tamra*) or other G4-forming sequences (F21RT, F25CebT, F21CTAT, FmycT, Fkit1T, Fkit2T; see the Experimental Section and the Supporting Information).[23] The stabilization, which was measured by a FRET effect, was expressed as the increase in melting temperature of the labeled oligonucleotide ($\Delta T_{1/2}$) induced by the ligand. Addition of an unlabeled DNA competitor (for example, duplex DNA) enables one to evaluate the selectivity for the targeted quadruplex structure.

The FRET melting data, summarized in Figure 1, indicate little or no stabilizing effect of the free organic ligands (BisQ, tBisQ, and tMebip), thereby confirming the crucial effect of the metallic cation, as previously observed.[9] Remarkably, compared with the corresponding Pt^{2+} and Cu^{2+} complexes, Pd^{2+} derivatives are clearly the most efficient at

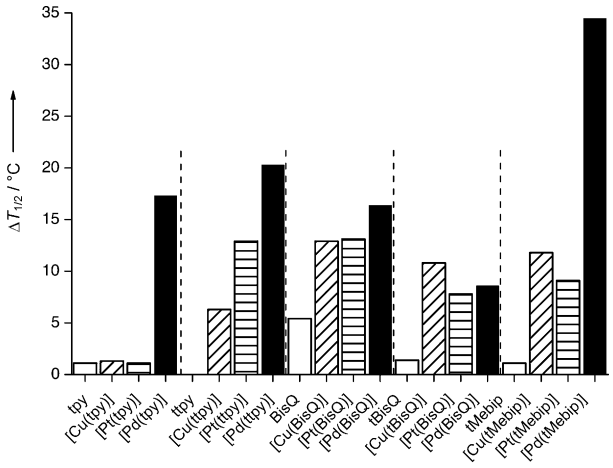

Figure 1. FRET melting stabilization ($\Delta T_{1/2}$ in °C) of the human telomeric sequence F21T (0.2 μM) in lithium cacodylate buffer (10 mM), KCl (10 mM), and LiCl (90 mM) in the presence of metal complexes or the corresponding free ligand (5 equiv). Ligand: white, Cu^{2+}: diagonal hatching, Pt^{2+}: horizontal hatching, Pd^{2+}: black.

 © 2011 Wiley-VCH Verlag GmbH & Co. KGaA, Weinheim

stabilizing human telomeric G4. The tpy series represents a striking example of the pronounced effect of Pd^{2+}. [Pd(tpy)] induces strong stabilization of the quadruplex structure ($\Delta T_{1/2} = +17.3\,°C$), whereas the two other tpy complexes exhibit a negligible effect ($\Delta T_{1/2} < +2\,°C$). Similarly, stabilization in the tMebip series is particularly impressive: $\Delta T_{1/2}$ for the Pd^{2+} complex almost reaches the limit of the test with a $\Delta T_{1/2}$ value of around $+35\,°C$, whereas $\Delta T_{1/2}$ values of around 10–12 °C are recorded for the Cu^{2+} and Pt^{2+} counterparts. The same trend was observed in the ttpy series, but to a lesser extent ($\Delta T_{1/2} = +20.3$, $+12.9$, $+6.3\,°C$ for Pd, Pt, and Cu derivatives, respectively). Conversely, the effect of palladium was much less striking in the BisQ and tBisQ series, for which the three complexes showed similar performances ($7–10\,°C < \Delta T_{1/2} < 14\,°C$). The hindrance of the aromatic surface of these ligands is likely to counterbalance the effect of the metallic cations, suggesting that in those cases the interaction is dominated by the aromatic ligand. On the other hand, the interaction is clearly governed by the nature of the metallic cation in the three other series (tpy, ttpy, and tMebip). The beneficial effects of cation and ligand are clearly additive in the case of [Pd(tMebip)], which appears to be the best candidate of the fifteen complexes studied.

Therefore, the tMebip series was similarly assayed for a wider spread of quadruplex-forming sequences of biological interest. The results shown in Figure 2 confirm the stronger

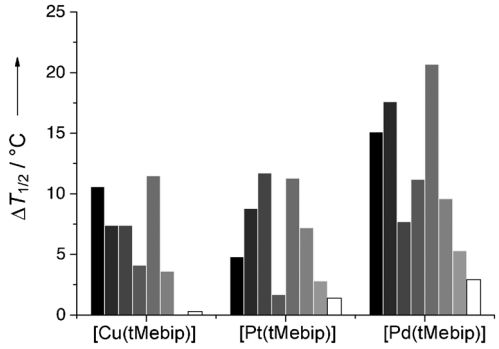

Figure 2. FRET melting stabilization ($\Delta T_{1/2}$ in °C) of the G4s F21T, F21RT, F25CebT, F21CTAT, FmycT, Fkit1T, Fkit2T (from black to light gray) and of the duplex FdxT (white) (0.2 μM) in lithium cacodylate buffer (10 mM), KCl (10 mM), and LiCl (90 mM) in the presence of tMebip complexes. [DNA] = 0.2 μM; [complexes] = 1 μM.

stabilization of almost all G4s by [Pd(tMebip)], compared with copper and platinum derivatives. Importantly, very low binding was observed when using the doubly labeled duplex (FdxT, 2.9 °C), revealing the strong preference of the compound for G4 structures. Notably, high quadruplex selectivity was also observed for the Cu^{2+} and Pt^{2+} complexes. The selectivity of [Pd(tMebip)], with regards to duplex structure, was also evaluated by competitive FRET melting using F21T and a 26 bp duplex (ds26) as a competitor. A high decrease was observed when adding the first dose (3 μM) of the duplex competitor, whereas the second dose (10 μM) did

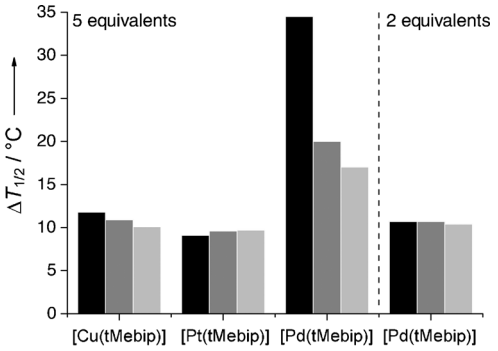

Figure 3. FRET melting stabilization ($\Delta T_{1/2}$ in °C) of the labeled G4 DNA human telomeric sequence F21T (0.2 μM) in lithium cacodylate buffer (10 mM), KCl (10 mM) + LiCl (90 mM), in the presence of increasing concentrations of competitor duplex DNA ds26 (0, 15, and 50 equiv, black to light gray), by 5 (left) and 2 equiv (right) of tMebip complexes.

not cause a further decrease in stabilization (Figure 3). The same trend was observed for all Pd^{2+} complexes, irrespective of the ligand (see Figure S1 in the Supporting Information), but not for the Pt^{2+} and Cu^{2+} complexes. Nevertheless, [Pd(tMebip)] retains a significant effect (+17 °C) under these conditions of harsh competition (50 equiv of duplex), and thus, remains the best candidate. The same experiment conducted at a lower concentration of [Pd(tMebip)] indicated that the decrease was abolished under these conditions of lower compound/DNA ratio, thereby suggesting that the excess compound may participate "nonspecifically" in the stabilization observed (Figure 3, left part).

This unusual behavior raises questions about the nature of the interaction and how to rationalize the effect of the palladium relative to the other cations, in particular, platinum. It could be hypothesized that a portion of the complex was bound externally, thus being easily redistributed on the competitor. In addition, metal coordination to DNA bases may occur during the experiment favored by the temperature increase. The $\Delta T_{1/2}$ value measured could thus result both from noncoordinative binding and from in situ coordination. To investigate further the nature of the interaction, in the case of Pd^{2+} and Pt^{2+} complexes, complementary experiments were conducted for the ttpy and tMebip families by using isothermal methods, namely, ESI-MS and UV/Vis spectroscopy.

ESI-MS: Mass spectrometry was used to characterize the amount of ligand bound to duplexes and G4 structures.[24] Furthermore, analysis of the masses of the complexes formed between [Pt(ttpy or tMebip)]/[Pd(ttpy or tMebip)] and DNA revealed a particular binding mode. Figure 4 shows a magnification of the complexes detected with the tetramolecular G4 Q1, $d[TGGGGT]_4$. Not shown is the signal of the free Q1 at charge state 5^-, with an average m/z of 1499.67. In the region corresponding to the complexes, three species can be distinguished: the association between DNA and the metal complex [Pt(ttpy or tMebip)]/[Pd(ttpy or tMebip)], the association between DNA and the aqua

 © 2011 Wiley-VCH Verlag GmbH & Co. KGaA, Weinheim

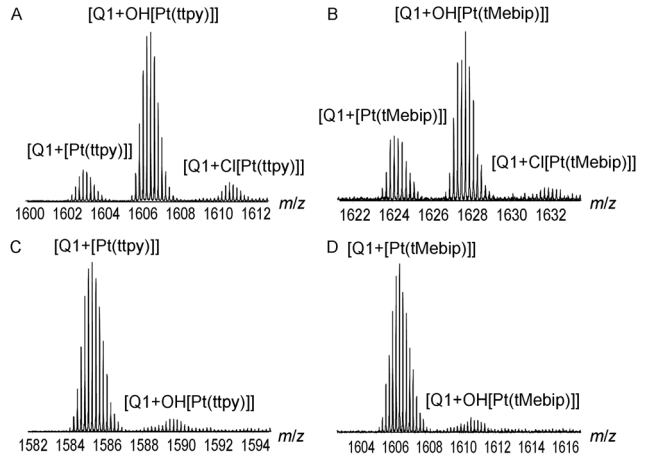

Figure 4. Nature of the 1:1 (DNA/ligand) complex of various metal derivatives ([Pt(ttpy)] (A), [Pt(tMebip)] (B), [Pd(ttpy)] (C), [Pd(tMebip)] (D)) with $[dTGGGGT]_4$ obtained 1 h after mixing. For platinum complexes (A and B) the binding of the aqua form (coordination of the Pt with OH) to Q1 is predominant. Minor species are complexed with the chloride form and direct coordination with DNA (neither OH nor Cl bound to the metallic cation). For palladium derivatives (C and D), direct coordination to the DNA is the major form, the aqua form is minor, and the chloride form is undetected.

form of the metal complex [PtOH(ttpy or tMebip)]/[PdOH(ttpy or tMebip)] and with its chlorido form [PtCl(ttpy or tMebip)]/[PdCl(ttpy or tMebip)].

In all cases, the free complex is in the chlorido form, as shown by high-resolution mass spectrometry (HRMS) analysis. For the two platinum complexes (Figure 4A and B), the major form bound to the DNA is, however, the aqua form (Cl^- is replaced by OH^-), but a few chlorido complexes associated with DNA are still observed. Another minor form is the complex directly bound to DNA, for which we conclude that one DNA base or residue occupies the fourth coordination site of Pt. The species with the chlorido and aqua forms are therefore interpreted as noncoordinative associations of the metal complexes with DNA (Scheme 5B and C), whereas species lacking Cl or OH are interpreted as coordinative associations involving coordination of the metal to DNA (Scheme 5D).

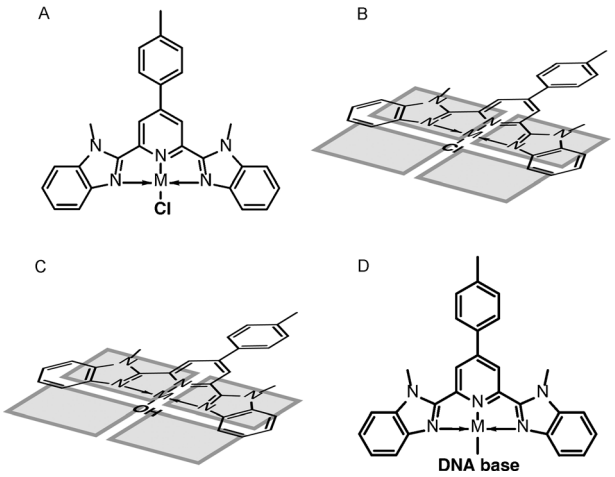

Scheme 5. Binding modes of [M(tMebip)] (M = Pt, Pd) observed by ESI-MS and time-dependent UV/Vis absorbance measurements. Complexes (A) can quickly π stack on a G-quartet (chlorido (B) and hydrolyzed (C) forms) and/or coordinate to DNA bases (D).

Experiments conducted after incubation of the Pt complexes with DNA for one day showed that the fraction of complex directly coordinated to DNA increased very slowly with time. For palladium complexes, however, hydrolysis and subsequent metalation of the DNA occur at a much faster rates than those for the platinum complexes and after incubation for 1 h most of the complexes are coordinated to DNA (Figure 4C and D). The aqua form is minor and the chloride form is absent. Because no ammonium cation is released from the G4 structure, opening of the G-quartet is unlikely to occur, and furthermore, this should be prevented by π stacking of the aromatic ligand. Thus, the guanines of the quadruplex core should be protected from metalation,[32] since their N7 position is engaged in Hoogsteen hydrogen bonding. Consequently, we hypothesized that complexes coordinated to thymines surrounding the G-quartet (Figure S2 in the Supporting Information). Indeed, Q1 possesses eight accessible thymines, the N3 of which is able to coordinate Pt^{2+} and Pd^{2+} cations when not engaged in base pairing.[33]

Mass spectrometry therefore allows the amount of metal complex bound coordinately and noncoordinately to the DNA to be quantified separately. Figure 5 summarizes the

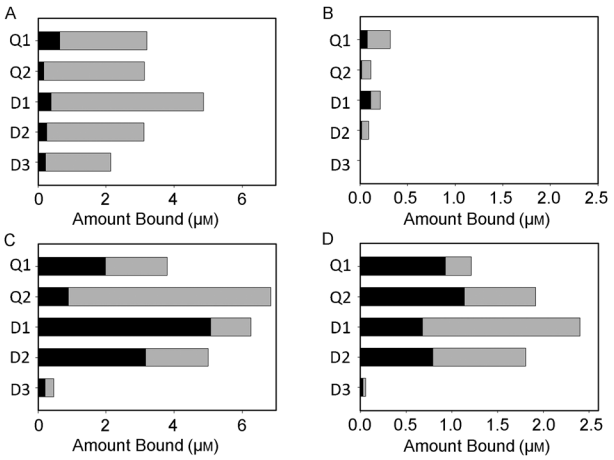

Figure 5. Amounts of metal complexes ([Pt(ttpy)] (A), [Pt(tMebip)] (B), [Pd(ttpy)] (C), [Pd(tMebip)] (D)) bound to different DNA G4s (Q1 = $[dTGGGGT]_4$, Q2 = human telomeric sequence $d(GGGTTA)_3GGG$) and duplexes (D1 = $(dCGCGGGCCCGCG)_2$, D2 = $(dCGCGAATTCGCG)_2$, D3 = $(dCGTAAATTTACG)_2$). The concentration was 4.8 μM of DNA and 8 μM of compound. The black bars correspond to the fraction of ligand directly coordinated to DNA and the grey bars correspond to the fraction of noncoordinately bound complexes (aqua and chlorido forms) 1 h after mixing.

quantification experiments with different quadruplexes (Q2 is the 21-nt human telomeric sequence and D1–D3 are 12 bp duplexes with decreasing GC content). Globally, the amount of compound bound to DNA was higher for ttpy complexes (Figure 5A and C) than for the tMebip counterparts (Figure 5B and D). The platinum derivative of

 © 2011 Wiley-VCH Verlag GmbH & Co. KGaA, Weinheim

tMebip, in particular, appears to be very poorly active (Figure 5B). However, the ratios of complexes bound noncoordinately and coordinately differ strongly: noncoordinating binding is largely predominant for Pt derivatives, whereas coordinate binding predominates for Pd derivatives. This is consistent with the faster coordination rate of the Pd series and confirms the formation of stable adducts with DNA. In all cases, no clear structural selectivity appears because both quadruplexes (Q1,2) and duplexes (D1,D2) are bound at a more or less comparable level. Nonetheless, binding to duplexes is strikingly dependent on the GC content, since AT-rich duplex D3 is very poorly bound, especially for palladium derivatives (Figure 5C and D). These observations are consistent with the preferential coordination of Pt^{2+} and Pd^{2+} to the N7 position of guanines,[34] and with the fast coordination rate of Pd complexes. Moreover, these tend to demonstrate that the palladium complexes bind externally in the major groove, where the N7 positions are accessible, and hence, do not insert into the duplex structure. Finally, the two Pd derivatives coordinate to the telomeric quadruplex Q2 more or less to the same extent (around 1 μM Figure 4C and D), but coordinative binding is much more prevalent for the ttpy complex (Figure 4C). In these cases, preferential coordination of the metal to the adenines present in the loops may be expected, as previously shown for Pt derivatives.[10]

In summary, the apparent affinity and structural selectivity should thus be interpreted in light of these two possible binding interactions, which may occur consecutively and/or concomitantly. Thus, if we assume that palladium complexes are stacked on one external quartet and locked into the structure by coordination to loop bases, this dual interaction should strongly stabilize the quadruplex structure. Consequently, it is not surprising that the greatest stabilization of quadruplexes is observed with palladium derivatives upon FRET melting because a large fraction of the complexes should be coordinately bound. However, the mass spectrometry results highlight that a comparison of FRET melting data for platinum and palladium complexes must be interpreted carefully, since the nature of the interaction (noncoordinative vs. coordinative) with DNA evolves with time and the ratio of noncoordinative versus coordinative binding can be modified by the temperature increase. Additionally, coordinative and noncoordinative binding modes should contribute differently to the apparent stabilization of G4s, depending on their respective fraction and $\Delta H_{binding}$. For the same reasons, the binding of palladium derivatives to duplex DNA is difficult to evaluate because 1) it is strongly sequence dependant and seems to occur without insertion into the duplex; 2) it is not necessarily a stabilizing interaction,[34b] and hence, may not be easily detectable by FRET melting; and 3) the fast coordination kinetics of palladium may favor coordination to duplexes under the ESI-MS conditions (a DNA concentration that is 24-fold higher than that in FRET melting and no competition with quadruplexes).

Time-dependent UV/Vis absorbance spectra: In an attempt to gain further insight into the coordination capability of the two series, the kinetics of coordination to DNA were followed by UV/Vis spectroscopy measurements, as previously described for [Pt(tpy)] complexes.[35] The absorption spectrum of [Pd(tMebip)] has a broad band with two local maxima at 330 and 400 nm, corresponding to the ligand-centered band (Figure 6). In the tail of this band, the weak contribution lying in the visible region is assigned to the metal-to-ligand charge-transfer band (MLCT).[36] Indeed this contribution cannot be the result of a metal centered d–d transition because it appears at a wavelength higher than 400 nm and is characterized by a low intensity.[37] The addition of telomeric quadruplex DNA [22AG, 5′-$AG_3(T_2AG_3)_3$-3′] (1 equiv) resulted in moderate hypochromism, suggesting π stacking of the complex, presumably on a G4. After this initial step, the spectrum further evolved over time with prominent hyperchromism of the ligand band, displaying a maximum at 330 nm. Concomittantly, the MLCT band increased in intensity and was slightly redshifted, while one isosbestic point common to all curves remained at 425 nm. This indicates the existence of interconversion between two species and agrees with coordination of the complex to DNA, as evidenced by the ESI-MS data. Indeed, the substitution of an electron-withdrawing atom (chlorine) with a neutral donor (nitrogen lone pair from a DNA base) can increase the electron density of the metal center, and therefore, decrease the MLCT energy.[37–38] Finally, two other isosbestic points appeared successively (395 nm, plain lines (Figure 6, then 380 nm, short dashed lines), suggesting the existence of two reactions with dissimilar rate constants, which may correspond to two differently coordinated species.[39] In the case of [Pd(ttpy)], the addition of G4 DNA also resulted in a rapid change of the absorption spectrum of the complex (Figure S3 in the Supporting Information). A significant hypochromism of the ligand band also suggested direct stacking of the complex on G4. The time evolution of the system

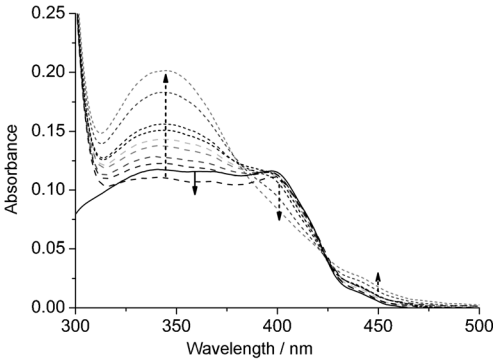

Figure 6. Change in absorption spectra during the interaction of [Pd(tMebip)] (10 μM) with 22AG (10 μM) in 10 mM lithium cacodylate, pH 7.2 buffer, and 100 mM KCl. Complex alone: solid line (solid arrow shows DNA addition). Successive times are 0, 50, 80, 160, 240 (black to light gray dashed lines), 320, 415, 1320, 3000 min (black to light gray short dashed lines). Dashed arrows indicate the kinetic evolution.

 © 2011 Wiley-VCH Verlag GmbH & Co. KGaA, Weinheim

was comparable to that of [Pd(tMebip)], that is, an increase in the absorbance of the ligand together with significant bathochromism of the MLCT. Overall, the UV data for [Pd(tMebip)] and [Pd(ttpy)] agree with the mass spectral data and suggest an interaction with quadruplex DNA through first stacking over a G4 and subsequently by fast coordination (on a minute timescale).

In contrast, no detectable immediate change occurred after the addition of 22AG to [Pt(tMebip)] (Figure S4 in the Supporting Information). Then the spectrum evolved in a similar fashion to that of [Pd(tMebip)], but to a much lower extent, with almost no change monitored in the MLCT band. Conversely, addition of 22AG to [Pt(ttpy)] led to rapid hypochromism followed by an increase in absorbance over time, along with the appearance of two simultaneous isosbestic points (350 and 415 nm; Figure S5 in the Supporting Information). Similar to [Pt(tMebip)], no significant modification of the MLCT was detected.

In vitro cytotoxicity: Finally, we evaluated the effect of tMebip and ttpy complexes on the growth of several cancer cell lines. For both families, Pd complexes were highly efficient (Table S1 in the Supporting Information). In particular, [Pd(ttpy)] strongly inhibited the proliferation of the three tested cell lines (KB, A549, and MCF7) with IC_{50} values in the nanomolar range (65–115 nM; Table S2 in the Supporting Information). This palladium complex was, in this regard, more efficient than [Pt(ttpy)], which has IC_{50} values in the micromolar range.[10] Whether the higher cytotoxicity of palladium derivatives is related to differences in the DNA interaction observed in vitro is not known and requires further investigations. Nevertheless, these results indicate that the novel compounds penetrate the cell membrane and exhibit a promising drug-like potential.

Conclusion

Using straightforward synthetic pathways, we prepared fifteen metal complexes, featuring three different metals, namely, copper(II), platinum(II), and palladium(II). Five structurally related tridentate N-donor ligands were used, including well known tpy and ttpy, and the already studied dibenzoterpyridine BisQ. To enhance the capability of metal complexes binding G4 DNA, two larger ligands (tBisQ and tMebip) were prepared. Unexpectedly, FRET melting experiments revealed, for the first time, a significant positive effect of palladium on the stabilization properties of the complexes for G4 DNA. We hypothesize that this striking difference between platinum and palladium complexes is due to a difference in the nature of the DNA binding interaction despite the fact that they share the same square-planar geometry. Consequently, ESI-MS and UV/Vis spectroscopy experiments were carried out and showed that, under the conditions examined, platinum complexes tended to predominantly bind G4 DNA in their aqua form by non-coordinative interactions, whereas palladium complexes coordinated DNA bases to a large extent in a short time. Notably, mass spectrometry revealed that, after incubation for 1 h at room temperature, a major fraction of the complexes involved palladated DNA. In addition, the palladium complexes may coordinate to thymines in the vicinity of the G4 core when no purine base is accessible. Overall, we demonstrated that tpy-like metal complexes could be finely tuned, by varying the nature of both metal and ligand, to target G4 by a multiple interaction based on noncoordinative π stacking and coordination to residues surrounding terminal G4s. This particular interaction may open up perspective for specifically targeting G4 structures exhibiting proper loop conformations and/or dynamics.

Experimental Section

General: ^{1}H and ^{13}C NMR spectra were recorded at 25 °C on a Bruker Avance 300 spectrometer using tetramethylsilane (TMS) as an internal standard. Deuterated $CDCl_3$ and [D_6]DMSO were purchased from SDS. The following abbreviations are used: singlet (s), doublet (d), triplet (t) and multiplet (m). Low-resolution ESI mass spectra were recorded on a micromass ZQ 2000 (Waters) instrument. High-resolution ESI mass spectra and elemental analyses were provided by the Institut de Chimie des Substances Naturelles (I.C.S.N., Gif-sur-Yvette, France). TLC analysis was carried out on silica gel (Merck 60F-254) plates with visualization at 254 and 366 nm. Preparative flash chromatography was carried out with Merck silica gel (Si 60, 40–63 μm). Reagents and chemicals were purchased from Sigma-Aldich, Acros, or Alfa-Aesar unless otherwise stated. Solvents were purchased from SDS. Melting points were recorded on a Kofler melting point apparatus and are uncorrected. UV/Vis spectra were recorded on a Secoman Uvikon XL spectrophotometer and fluorescence melting curves were recorded on a Stratageme Mx 3005P real-time PCR machine. Oligonucleotides purified by reversed-phase HPLC were purchased from Eurogentec (Belgium).

Preparation of palladium complexes: A solution of dichloro(1,5-cyclooctadiene)palladium (1.2 equiv) in a minimum amount of CH_2Cl_2 was added to a solution of ligand (1 equiv) in a minimum amount of DMF. The resulting yellow solution was stirred for 2–3 d at room temperature under argon and protected from light. The resulting suspension was filtered. The solid was washed with DMF, CH_2Cl_2, and then diethyl ether. The powder was then dried under vacuum.

Preparation of platinum complexes: Platinum complexes with tpy and ttpy were prepared as previously described.[9] Other complexes were prepared as follows:[31c] Potassium platinum(IV) chloride (1 equiv) and sodium tetrafluoroborate (2 equiv) were added to a solution of ligand in dry nitromethane. The mixture was heated at reflux for 48 h under argon and protected from light. The NaCl precipitate was removed by hot filtration. The product was precipitated by addition of diethyl ether (when necessary), filtered through a membrane (Schleicher & Schuell, 1 μm), washed with CH_2Cl_2 and diethyl ether, then dried under vacuum.

Preparation of copper complexes: A solution of copper nitrate (1.1 equiv) in a minimum amount of anhydrous acetonitrile was carefully added dropwise to a solution of the ligand (1 equiv) in a minimum amount of CH_2Cl_2 to form two immiscible layers. The biphasic solution was kept at 4 °C until complete discoloration of the upper phase (typically 1–3 days). Green needles were filtered off; washed carefully with acetonitrile, CH_2Cl_2, and diethyl ether; then dried under vacuum.

Synthesis of 1: The procedure for the synthesis of **1** was adapted from literature.[25] Chelidamic acid (3 g, 15 mmol) and *N*-methylphenylenediamine (3.4 mL, 30 mmol) in polyphosphoric acid (55 g) were added to a 250 mL round-bottomed flask to afford a red viscous solution that was stirred under argon at 250 °C. After 48 h, the solution was poured (hot) into cold water (300 mL) under vigorous stirring. The blue solid was col-

 © 2011 Wiley-VCH Verlag GmbH & Co. KGaA, Weinheim

lected by filtration, taken up into aqueous Na_2CO_3 (10%) at 110°C for 15 min, then filtered off. The solid was suspended in water (300 mL) and the pH was adjusted to four. The foamy solid was collected again by filtration. It was then recrystallized from hot DMSO by adding water until the solution became cloudy. After the solution cooled, compound **1** was recovered as white needles (4.4 g, 12.38 mmol, 83%). M.p. 135°C (decomp); ^{1}H NMR (300 MHz, [D$_6$]DMSO): δ=11.40 (br s 1H), 7.84–7.58 (m, 2H), 7.47–7.12 (m, 4H), 4.25 ppm (s, 6H); ^{13}C NMR (75 MHz, [D$_6$]DMSO): δ=165.5, 150.2, 149.5, 140.7, 136.7, 123.7, 123.0, 119.0, 113.1, 111.2, 32.7 ppm.

Synthesis of 2: Compound **2** was prepared from **1** as described in the literature.[26]

Synthesis of tMebip: Compound **2** (100 mg, 0.24 mmol), 4-tolylboronic acid (32.6 mg, 0.24 mmol), potassium acetate (99 mg, 0.72 mmol), and tetrakis(triphenylphosphine)palladium (17.3 mg, 0.015 mmol) were added to a degassed solution of THF (80 mL) and water (35 mL) to give a brown solution that was heated at reflux under argon for 24 h. The reaction mixture was allowed to cool slowly to room temperature. Light brown needles were filtered off. Recrystallization from THF/water afforded pure tMebip (66.8 mg, 65% yield). M.p. 215°C (dec); ^{1}H NMR (300 MHz, [D$_6$]DMSO): δ=8.64 (s, 2H), 7.89 (s, 2H), 7.76 (dd, J=24.2, 7.9 Hz, 4H), 7.51–7.23 (m, 6H; Ar), 4.30 (s, 6H), 2.42 ppm (s, 3H); ^{13}C NMR (75 MHz, CDCl$_3$): δ=150.7, 150.7, 150.2, 142.8, 140.1, 137.4, 134.2, 130.1, 127.4, 123.8, 123.1, 123.0, 120.4, 110.2, 32.8, 21.5 ppm; HRMS: m/z calcd for $C_{28}H_{23}N_5Na$: 452.185; found: 452.1869.

[Pd(tMebip)]: Green–yellow powder (48%); ^{1}H NMR (300 MHz, [D$_6$]DMSO): δ=8.43 (s, 2H), 8.17 (d, J=8.0 Hz, 2H), 7.84 (d, J=8.2 Hz, 2H), 7.59 (d, J=8.0 Hz, 2H), 7.35 (m, 6H), 4.19 (s, 6H), 2.53 ppm (s, 3H); LRMS: m/z: 571 [M+H$^+$]; HRMS: m/z calcd for $C_{28}H_{23}N_5ClPd$: 574.0676; found: 570.0504.

[Pt(tMebip)]: Dark orange powder (16%); ^{1}H NMR (300 MHz, [D$_6$]DMSO): δ=8.21 (s, 2H), 8.06 (d, J=7.5 Hz, 2H), 7.67–7.45 (m, J=7.9 Hz, 4H), 7.39 (dt, J=24.9 Hz, 4H), 7.14 (d, 2H), 4.12 (s, 6H), 2.50 ppm (s, 3H); LRMS: m/z: 661.2 [M+H$^+$]; HRMS: m/z calcd for $C_{28}H_{23}N_5{}^{35}ClPt$: 659.1290; found: 659.1319.

[Cu(tMebip)]: Green needles (42%); LRMS (in presence of formic acid): m/z: 553.9 [M+H$^+$], 537.0 [M−NO$_3$+formic acid], 526.9 [M−NO$_3$+2OH], 491.9 [M−NO$_3$]; HRMS: m/z calcd for $C_{28}H_{23}N_6O_3Cu$: 554.1128; found: 554.1112.

Synthesis of BisQ: Iron powder (1120 mg, 20.05 mmol) was added to a solution *o*-nitrobenzaldehyde (303 mg, 2.005 mmol) in ethanol (10 mL) followed by 0.1 N aqueous hydrochloric acid (4 mL, 0.400 mmol). The resulting mixture was vigorously stirred at 95°C (oil bath). When TLC analysis showed complete reduction of *o*-nitrobenzaldehyde (after approximately 2 h 30 min), 2,6-diacetylpyridine (135 mg, 1.003 mmol) and potassium hydroxide (337 mg, 6.02 mmol) were added. The reaction mixture was stirred at 95°C for 16 h, then cooled to RT, diluted with CH_2Cl_2 (100 mL), and filtered through a pad of Celite. The solution was concentrated and the residue was purified by column chromatography on silica gel (gradient CH_2Cl_2/MeOH: 100/0 to 90/10) to afford BisQ as a white solid (250 mg, 0.750 mmol, 75%). M.p. 216–218°C; ^{1}H NMR (300 MHz, CDCl$_3$): δ=8.86 (d, J=8.6 Hz, 2H), 8.78 (d, J=7.8 Hz, 2H), 8.36 (d, J=8.7 Hz, 2H), 8.22 (d, J=8.4 Hz, 2H), 8.08 (t, J=7.8 Hz, 1H), 7.90 (d, J=8.1 Hz, 2H), 7.76 (t, J=7.5 Hz, 2H), 7.58 ppm (t, J=7.4 Hz, 2H); ^{13}C NMR (75 MHz, CDCl$_3$): δ=156.3, 155.7, 148.1, 138.1, 136.9, 130.0, 129.7, 128.5, 127.8, 126.9, 122.2, 119.2 ppm;. LRMS: m/z: 334.2 [M+H$^+$]; HRMS: m/z calcd for $C_{23}H_{16}N_3$: 334.1344; found: 334.1350.

[Pd(BisQ)]: Brown–yellow powder (84%); ^{1}H NMR (300 MHz, [D$_6$]DMSO): δ=9.40 (s, 1H), 9.04 (s, 1H), 8.81 (d, J=16.1 Hz, 2H), 8.70 (d, J=7.6 Hz, 2H), 8.57 (d, J=7.1 Hz, 1H), 8.16 (dd, J=17.3, 8.0 Hz, 2H), 8.04 (s, 2H), 7.83 (s, 2H), 7.66 ppm (s, 2H); LRMS: m/z (%): 465 (50) [M−Cl+CN]$^+$, 439 (100) [M−Cl]$^+$, 474 (50) [M]$^+$; HRMS: m/z calcd for $C_{23}H_{16}N_3ClPd$: 475.0068; found: 475.0061.

[Pt(BisQ)]: Dark orange powder (21%); ^{1}H NMR (300 MHz, [D$_6$]DMSO): δ=8.90 (d, J=8.4 Hz, 2H), 8.76 (d, J=7.5 Hz, 2H), 8.62 (d, J=8.6 Hz, 2H), 8.26 (t, J=7.4 Hz, 1H), 8.17 (d, J=8.2 Hz, 2H), 8.10 (d, J=7.8 Hz, 2H), 7.87 (t, J=7.0 Hz, 2H), 7.70 ppm (d, J=7.1 Hz, 2H); LRMS: m/z (%): 527 (100) [M−Cl]$^+$, 555 (80) [M−Cl+CN]$^+$, 563.9 (5) [M+H$^+$]; HRMS: m/z calcd for $C_{23}H_{15}N_3NaClPt$: 586.0500; found: 586.0519.

[Cu(BisQ)]: Green needles (52%); LRMS: m/z (%): 458.04 (100) [M+H$^+$], 396.0 (80) [M−2NO$_3$]$^+$; HRMS: m/z calcd for $C_{23}H_{15}N_4O_3{}^{63}Cu$: 458.0440; found: 458.0435.

Synthesis of 3: In a 250 mL flask, quinaldic acid (4.12 g, 23.79 mmol) was dissolved in MeOH (40 mL). Concentrated H_2SO_4 (1 mL) was added and the mixture was heated at reflux for 16 h. After cooling to RT, the mixture was neutralized with a saturated aqueous solution of $NaHCO_3$ and extracted with CH_2Cl_2 (3×100 mL). The organic phases were combined, dried with $MgSO_4$, and evaporated to afford **3** as a white solid (3.97 g, 21.21 mmol, 89%). M.p. 83°C (81–83°C lit. [40]); ^{1}H NMR (300 MHz, CDCl$_3$): δ=8.32 (d, J=8.3 Hz, 2H), 8.21 (d, J=8.5 Hz, 1H), 7.89 (d, J=8.2 Hz, 1H), 7.80 (t, J=7.7 Hz, 1H), 7.66 (t, J=7.5 Hz, 1H), 4.09 ppm (s, 3H); ^{13}C NMR (75 MHz, CDCl3): δ=166.0, 147.9, 147.5, 137.33, 130.7, 130.3, 129.4, 128.6, 127.6, 121.0, 52.2 ppm; LRMS: m/z (%): 188.2 (100) [M+H$^+$].

Synthesis of 4:[40] Solid *t*BuOK (1.559 g, 13.89 mmol) was slowly added to a solution of **3** (2 g, 10.68 mmol) in ethyl acetate (35 mL). The mixture was stirred for 15 min at RT and then quenched with H_2O (60 mL). The organic layer was separated and the aqueous phase was extracted with EtOAc (3×50 mL). The organic phases were combined, dried with $MgSO_4$, and evaporated. The residue was purified by flash chromatography (EtOAc/cyclohexane, 1:4) to afford **4** as an off-white paste (2.06 g, 8.47 mmol, 79%). ^{1}H NMR (300 MHz, CDCl$_3$): δ=8.27 (d, J=8.3 Hz, 1H), 8.16 (t, J=7.2 Hz, 2H), 7.88 (d, J=8.2 Hz, 1H), 7.79 (t, J=7.2 Hz, 1H), 7.64 (t, J=7.5 Hz, 1H), 4.36 (s, 2H), 4.22 (q, J=7.2 Hz, 2H), 1.26 ppm (t, J=7.2 Hz, 3H).

Synthesis of 5:[40] In a 250 mL flask, compound **4** (2.06 g, 7.95 mmol) was dissolved in dioxane (20 mL). HCl (1 M, 20 mL) was added and the solution was stirred at 100°C for 16 h, then it was concentrated under reduced pressure. The residual aqueous phase was extracted with EtOAc (3×50 mL). The organic phases were combined, washed with a saturated aqueous solution of $NaHCO_3$, dried with $MgSO_4$, and evaporated. The residue was purified by chromatography on a small silica gel column to afford **5** as a white solid (954 mg, 5.57 mmol, 70%). M.p. 49°C; ^{1}H NMR (300 MHz, CDCl$_3$): δ=8.27 (d, J=8.5 Hz, 1H), 8.20 (d, J=8.5 Hz, 1H), 8.13 (d, J=8.5 Hz, 1H), 7.87 (d, J=8.1 Hz, 1H), 7.79 (t, J=7.7 Hz, 1H), 7.65 (t, J=7.5 Hz, 1H), 2.88 (s, 3H) ppm; ^{13}C NMR (75 MHz, CDCl$_3$): δ=200.7, 153.2, 147.2, 136.9, 130.6, 130.0, 129.6, 128.6, 127.7, 118.0, 25.6 ppm; LRMS: m/z: 194.2 [M+Na$^+$].

Synthesis of tBisQ: Compound **5** (100 mg, 0.584 mmol) was added in a solution of 4-methylbenzaldehyde (35.1 mg, 0.292 mmol), potassium hydroxyde (32,8 mg, 0,584 mmol), and aqueous ammonia (28%; 0.73 mL, 33.7 mmol) in EtOH (5 mL). The mixture was heated for 24 h at 100°C into a sealed tube. After the mixture had been cooled to RT, a white precipitate was filtered, washed with MeOH and Et$_2$O, and dried to afford the first batch of product. The filtrate was concentrated and the residue was purified by column chromatography on silica gel (cyclohexane/CH_2Cl_2 from 50/50 to 0/100) to afford a second batch of product. Purification afforded tBisQ as a white powder (67 mg, 0.059 mmol, 54%). M.p. 244–246°C; ^{1}H NMR (300 MHz, CDCl$_3$): δ=9.02 (s, 2H), 8.89 (d, J=8.6, 2H), 8.36 (d, J=8.6, 2H), 8.25 (d, J=8.4, 2H), 7.97–7.83 (m, 4H), 7.77 (t, J=7.7, 2H), 7.59 (t, J=7.5, 2H), 7.39 (d, J=7.9, 2H), 2.48 ppm (s, 3H); ^{13}C NMR (75 MHz, CDCl$_3$): δ=156.5, 156.2, 150.4, 148.1, 139.2, 136.8, 135.9, 130.0, 129.9, 129.7, 128.5, 127.4, 126.9, 119.9, 119.5, 21.5 ppm; LRMS: m/z: 424.1 [M+H]$^+$; HRMS: m/z calcd for $C_{30}H_{21}N_3Na$: 446.1633; found: 446.1623.

[Pd(tBisQ)]: Yellow powder (40%); ^{1}H NMR (300 MHz, [D$_6$]DMSO): δ=9.38 (s, 1H), 9.00–8.85 (m, 4H), 8.56 (d, J=7.2 Hz, 2H), 8.16–7.98 (m, 4H), 7.86 (t, J=8.7 Hz, 4H), 7.66 (t, J=7.5 Hz, 2H), 7.41 (d, J=7.9 Hz, 2H), 2.43 ppm (s, 3H); LRMS (in presence of acetonitrile): m/z: 566.0 [M+H$^+$], 456.1 [M−Cl+CN+H$^+$]; HRMS: m/z calcd for $C_{30}H_{22}N_3ClPd$: 565.0537; found: 565.0537.

[Pt(tBisQ)]: Red powder (94%); ^{1}H NMR (300 MHz, [D$_6$]DMSO): δ=9.30 (d, J=8.6 Hz, 2H), 8.81 (s, 4H), 8.64 (d, J=8.2 Hz, 2H), 7.95 (d, J=7.5 Hz, 4H), 7.77 (dt, J=14.6, 7.0 Hz, 4H), 7.19 (d, J=7.7 Hz, 2H),

 © 2011 Wiley-VCH Verlag GmbH & Co. KGaA, Weinheim

2.34 ppm (s, 3H); LRMS (in presence of acetonitrile): *m/z*: 654.1 [*M*+H$^+$]; HRMS: *m/z* calcd for $C_{30}H_{21}N_3{}^{35}Cl^{196}Pt$: 654.1073; found: 654.1124.

[Cu(tBisQ)]: Green needles (65%); LRMS: *m/z* (%): 548.1 (15) [*M*+H$^+$],486.1 (100) [*M*−2NO$_3$]$^+$; HRMS: *m/z* calcd for $C_{30}H_{21}N_3{}^{63}Cu$: 486.1031; found: 486.1038.

[Pd(tpy)]: Yellow powder (99%); m.p. >260°C (decomp); ^{1}H NMR (300 MHz, [D$_6$]DMSO): δ=8.79–8.58 (m, 7H), 8.47 (t, *J*=7.8 Hz, 2H), 7.88 (t, *J*=6.5 Hz, 2H) ppm; LRMS (in presence of acetonitrile): *m/z*: 376 [*M*+H$^+$], 365.0 [*M*−Cl+CN+H$^+$]; HRMS: *m/z* calcd for $C_{15}H_{11}N_3{}^{35}Cl^{108}Pd$: 375.9680; found: 375.9668.

[Pd(ttpy)]: Orange powder (78%); m.p. >260°C (decomp); ^{1}H NMR (300 MHz, [D$_6$]DMSO): δ=8.95 (d, *J*=5.4 Hz, 2H), 8.86 (d, *J*=7.8 Hz, 2H), 8.71 (d, *J*=5.4 Hz, 2H), 8.50 (d, *J*=8.0 Hz, 2H), 8.13 (d, *J*=8.1 Hz, 2H), 7.89 (d, *J*=6.8 Hz, 2H), 7.49 (d, *J*=8.2 Hz, 2H), 2.45 (s, 3H) ppm; LRMS (in presence of acetonitrile): *m/z*: 466.0 [*M*+H$^+$], 455.1 [*M*−Cl+CN+H$^+$]; HRMS: *m/z* calcd for $C_{22}H_{17}N_3{}^{35}ClPd$: 464.0146; found: 464.0168.

FRET melting: FRET melting assays were performed with oligonucleotides that mimic the human telomeric sequence, as well as other quadruplex-forming oligonucleotides (25Ceb, 21CTA, c-Myc, c-Kit1, c-Kit2), and the control duplex ds26, equipped with FRET partners at each extremity (see sequences given in the Supporting Information). Measurements were made with excitation at 492 nm and detection at 516 nm in a 10 mM lithium cacodylate pH 7.2 buffer supplemented with 10 mM KCl and 90 mM LiCl.

ESI mass spectrometry: ESI-MS experiments were performed on a SolariX 9.4T FTICR mass spectrometer (Bruker Daltonics, Bremen, DE). The electrospray ion source was used in negative ion mode with a capillary voltage of −3.1 kV. The source parameters were tuned so as to minimize collisional activation (source pressure 3.1 mbar, skimmer at −20 V). The instrument was externally calibrated with sodium iodide (<1 ppm accuracy). High-resolution mass spectra and comparison with theoretical isotopic patterns were performed to unambiguously assign the nature of the observed complexes. Oligodeoxynucleotides d-CGTAAATTTACG (3644.45 Da), d-CGCGAATTCGCG (3646.44 Da), d-CGCGGGCCCGCG (3678.40 Da), d-TGGGGT (1863.26 Da), and d-(GGGTTA)$_3$GGG (6653.35 Da) were purchased from Eurogentec (Angleur, Belgium) and used without further purification. Duplex and quadruplex solutions were prepared in ammonium acetate (150 mM) according to previous reports.[24] The quantification of free DNA and complexes was performed on the most abundant charge state (5$^-$).

Molecular modeling: Optimized structures of OH-Pt/[Pd(tMebip)] and Thymine-Pt/[Pd(tMebip)] were obtained by using DFT with the hybrid functional B3LYP and the 6–1G(d) basis set. The LANL2DZ effective core potential was used for Pt and Pd. The molecular model of the complex [Pd(tMebip)] to the quadruplex (TGGGGT)$_4$ (Q1) was obtained as follows: The starting structure of Q1 was obtained after 10 ns of in vacuo molecular dynamics by using a modified AMBER parm99 force field.[41] The ligand was manually docked to the 3′ side of the G4 on top of the last G tetrad. One of the thymines of Q1 was coordinated to [Pd(tMebip)] and the complex was geometrically optimized prior to 1 ns molecular dynamics calculations.

UV kinetics: Absorbance spectra were recorded on an Uvikon XL Secomam spectrophotometer. Absorbance spectra were recorded from 300 to 500 nm with 10 μM ligand in 10 mM lithium cacodylate pH 7.2 buffer supplemented with 100 mM KCl. Local maxima were determined by using a second derivative method with quadratic Savitsky-Golay smoothing. After addition of 1 equiv of quadruplex-folded telomeric DNA, absorbance spectra were recorded over time.

In vitro cytotoxicity: The human cell lines originated from ATCC, except when otherwise stated. The human cell lines KB (nasopharynx epidermoid carcinoma) were grown in D-MEM medium supplemented with 10% fetal calf serum (InVitrogen) in the presence of 100 UI mL^{-1} penicillin, 100 μg mL^{-1} streptomycin, and 1.5 μg mL^{-1} fungizone in a 75 mL flask under 5% CO_2, whereas MCF7 cells (breast adenocarcinoma) were grown in RPMI medium. Resistant MCF7 cells were obtained by prolonged treatment with adriamycin. Cells were plated in 96-well tissue culture plates in medium (200 μL) and treated 24 h later with compounds dissolved in DMSO using a Biomek 3000 (Beckman) instrument. Controls received the same volume of DMSO (1% final volume). After 72 h exposure, MTS reagent (Celltiter 96Aqueous One solution, Promega) was added and incubated for 3 h at 37°C: the absorbance was monitored at 490 nm and results were expressed as the inhibition of cell proliferation calculated as the ratio {[1-(OD490 treated/OD490 control)]×100} in triplicate experiments. For IC_{50} determinations (50% inhibition of cell proliferation), cells were incubated for 72 h by following the same protocol with compound concentrations ranging from 0.5 nM to 10 μM in separate duplicate experiments. The antiproliferative activities of complexes were determined against a panel of human tumor cell lines. First percentages of inhibition of both compounds were evaluated at a concentration of 10^{-5} M^{-1} the ligand. [Pd(ttpy)] appeared to be a much more potent ligand and IC_{50} values were determined.

Acknowledgements

We gratefully acknowledge the generous financial support from the Centre National de la Recherche Scientifique and the Institut Curie (joint Ph.D. fellowship to E.L.), the Agence Nationale de la Recherche (ANR) for financial support to F.H., J.L.M., and M.P.T.F. (ANR-09-BLAN-0355 "G4Toolbox"), the Conseil régional d'Aquitaine and Association pour la Recherche sur le Cancer (ARC) (to J.L.M.), and the Fonds de la Recherche Scientifique-FNRS (V.G. is a FNRS research associate; F.R. is a FNRS scientific collaborator at the research associate level). We sincerely thank Dr. Sophie Bombard for fruitful discussions.

[1] a) J. L. Huppert, S. Balasubramanian, *Nucleic Acids Res.* **2007**, *35*, 406–413; b) A. K. Todd, *Methods* **2007**, *43*, 246–251.
[2] M. Gellert, M. N. Lipsett, D. R. Davies, *Proc. Natl. Acad. Sci. USA* **1962**, *48*, 2013–2018.
[3] H. J. Lipps, D. Rhodes, *Trends Cell Biol.* **2009**, *19*, 414–422.
[4] a) S. Balasubramanian, S. Neidle, *Curr. Opin. Chem. Biol.* **2009**, *13*, 345–353; b) D. Monchaud, M.-P. Teulade-Fichou, *Org. Biomol. Chem.* **2008**, *6*, 627–636.
[5] N. H. Campbell, M. Patel, A. B. Tofa, R. Ghosh, G. N. Parkinson, S. Neidle, *Biochemistry* **2009**, *48*, 1675–1680.
[6] a) S. Cosconati, L. Marinelli, R. Trotta, A. Virno, L. Mayol, E. Novellino, A. J. Olson, A. Randazzo, *J. Am. Chem. Soc.* **2009**, *131*, 16336–16337; b) S. Cosconati, L. Marinelli, R. Trotta, A. Virno, S. De Tito, R. Romagnoli, B. Pagano, V. Limongelli, C. Giancola, P. G. Baraldi, L. Mayol, E. Novellino, A. Randazzo, *J. Am. Chem. Soc.* **2010**, *132*, 6425–6433; c) Q. Li, J. Xiang, X. Li, L. Chen, X. Xu, Y. Tang, Q. Zhou, L. Li, H. Zhang, H. Sun, A. Guan, Q. Yang, S. Yang, G. Xu, *Biochimie* **2009**, *91*, 811–819.
[7] B. Rosenberg, L. vanCamp, J. E. Trosko, V. H. Mansour, *Nature* **1969**, *222*, 385–386.
[8] S. N. Georgiades, N. H. Abd Karim, K. Suntharalingam, R. Vilar, *Angew. Chem.* **2010**, *122*, 4114–4128; *Angew. Chem. Int. Ed.* **2010**, *49*, 4020–4034.
[9] H. Bertrand, D. Monchaud, A. D. Cian, R. Guillot, J.-L. Mergny, M.-P. Teulade-Fichou, *Org. Biomol. Chem.* **2007**, *5*, 2555–2559.
[10] H. Bertrand, S. Bombard, D. Monchaud, E. Talbot, A. Guedin, J.-L. Mergny, R. Grunert, P. J. Bednarski, M.-P. Teulade-Fichou, *Org. Biomol. Chem.* **2009**, *7*, 2864–2871.
[11] a) E. Wong, C. M. Giandomenico, *Chem. Rev.* **1999**, *99*, 2451–2466; b) E. R. Jamieson, S. J. Lippard, *Chem. Rev.* **1999**, *99*, 2467–2498; c) J. Kozelka, F. Legendre, F. Reeder, J.-C. Chottard, *Coord. Chem. Rev.* **1999**, *190–192*, 61–82.
[12] I. Eryazici, C. N. Moorefield, G. R. Newkome, *Chem. Rev.* **2008**, *108*, 1834–1895.
[13] J. L. Butour, S. Wimmer, F. Wimmer, P. Castan, *Chem.-Biol. Interact.* **1997**, *104*, 165–178.

 © 2011 Wiley-VCH Verlag GmbH & Co. KGaA, Weinheim

[14] a) M. Cusumano, A. Giannetto, *J. Inorg. Biochem.* **1997**, *65*, 137–144; b) Y. Ma, C. S. Day, U. Bierbach, *J. Inorg. Biochem.* **2005**, *99*, 2013–2023.
[15] a) M. Shoukry, H. Hohmann, R. van Eldik, *Inorg. Chim. Acta* **1992**, *198–200*, 187–192; b) A. Garoufis, S. K. Hadjikakou, N. Hadjiliadis, *Coord. Chem. Rev.* **2009**, *253*, 1384–1397.
[16] J. V. Burda, M. Zeizinger, J. Leszczynski, *J. Chem. Phys.* **2004**, *120*, 1253–1262.
[17] A. Garoufis, S. K. Hadjikakou, N. Hadjiliadis in *Metallotherapeutic Drugs and Metal-Based Diagnostic Agents: The Use of Metals in Medicine* (Eds.: M. Gielen, E. R. T. Tiekink), Wiley, New York, **2005**, pp. 399–419.
[18] J. E. Reed, A. J. P. White, S. Neidle, R. Vilar, *Dalton Trans.* **2009**, 2558–2568.
[19] T. Yutaka, S. Obara, S. Ogawa, K. Nozaki, N. Ikeda, T. Ohno, Y. Ishii, K. Sakai, M.-a. Haga, *Inorg. Chem.* **2005**, *44*, 4737–4746.
[20] B. M. O'Neill, J. E. Ratto, K. L. Good, D. C. Tahmassebi, S. A. Helquist, J. C. Morales, E. T. Kool, *J. Org. Chem.* **2002**, *67*, 5869–5875.
[21] a) G. Li, J. Huang, M. Zhang, Y. Zhou, D. Zhang, Z. Wu, S. Wang, X. Weng, X. Zhou, G. Yang, *Chem. Commun.* **2008**, 4564–4566; b) J. Huang, G. Li, Z. Wu, Z. Song, Y. Zhou, L. Shuai, X. Weng, X. Zhou, G. Yang, *Chem. Commun.* **2009**, 902–904; c) A. K. Jain, V. V. Reddy, A. Paul, M. K, S. Bhattacharya, *Biochemistry* **2009**, *48*, 10693–10704; d) S. Bhattacharya, P. Chaudhuri, A. K. Jain, A. Paul, *Bioconjugate Chem.* **2010**, *21*, 1148–1159.
[22] P. Wang, C.-H. Leung, D.-L. Ma, S.-C. Yan, C.-M. Che, *Chem. Eur. J.* **2010**, *16*, 6900–6911.
[23] a) J. L. Mergny, J. C. Maurizot, *ChemBioChem* **2001**, *2*, 124–132; b) A. De Cian, L. Guittat, M. Kaiser, B. Sacca, S. Amrane, A. Bourdoncle, P. Alberti, M. P. Teulade-Fichou, L. Lacroix, J. L. Mergny, *Methods* **2007**, *42*, 183–195.
[24] F. Rosu, E. De Pauw, V. Gabelica, *Biochimie* **2008**, *90*, 1074–1087.
[25] P. Froidevaux, J. M. Harrowfield, A. N. Sobolev, *Inorg. Chem.* **2000**, *39*, 4678–4687.
[26] P. K. Iyer, J. B. Beck, C. Weder, S. J. Rowan, *Chem. Commun.* **2005**, 319–321.
[27] D. Knapton, M. Burnworth, S. J. Rowan, C. Weder, *Angew. Chem.* **2006**, *118*, 5957–5961; *Angew. Chem. Int. Ed.* **2006**, *45*, 5825–5829.
[28] a) J. R. B. Gomes, *J. Phys. Chem. A* **2009**, *113*, 1628–1634; b) L. Ukhin, E. Belov, *Russ. Chem. Bull.* **2008**, *57*, 418–421.
[29] A.-H. Li, E. Ahmed, X. Chen, M. Cox, A. P. Crew, H.-Q. Dong, M. Jin, L. Ma, B. Panicker, K. W. Siu, A. G. Steinig, K. M. Stolz, P. A. R. Tavares, B. Volk, Q. Weng, D. Werner, M. J. Mulvihill, *Org. Biomol. Chem.* **2007**, *5*, 61–64.
[30] F. Kröhnke, *Synthesis* **1976**, *1976*, 1–24.
[31] a) S. D. Cummings, *Coord. Chem. Rev.* **2009**, *253*, 449–478; b) Q.-Z. Yang, L.-Z. Wu, Z.-X. Wu, L.-P. Zhang, C.-H. Tung, *Inorg. Chem.* **2002**, *41*, 5653–5655; c) X. Liu, E. J. L. McInnes, C. A. Kilner, M. Thornton-Pett, M. A. Halcrow, *Polyhedron* **2001**, *20*, 2889–2900.
[32] S. Redon, S. Bombard, M.-A. Elizondo-Riojas, J.-C. Chottard, *Biochemistry* **2001**, *40*, 8463–8470.
[33] a) J. Duguid, V. A. Bloomfield, J. Benevides, G. J. Thomas, *Biophys. J.* **1993**, *65*, 1916–1928; b) J. Ruiz, J. Lorenzo, L. Sanglas, N. Cutillas, C. Vicente, M. D. Villa, F. X. Avilés, G. López, V. Moreno, J. Pérez, D. Bautista, *Inorg. Chem.* **2006**, *45*, 6347–6360; c) A. Messere, E. Fabbri, M. Borgatti, R. Gambari, B. D. Blasio, C. Pedone, A. Romanelli, *J. Inorg. Biochem.* **2007**, *101*, 254–260.
[34] a) M.-H. Baik, R. A. Friesner, S. J. Lippard, *J. Am. Chem. Soc.* **2003**, *125*, 14082–14092; b) J. K. Barton in *Bioinorganic Chemistry* (Eds.: I. Bertini, H. B. Gray, S. J. Lippard, J. S. Valentine), University Press, Mill Valley, **1994**, pp. 455–504.
[35] C. S. Peyratout, T. K. Aldridge, D. K. Crites, D. R. McMillin, *Inorg. Chem.* **1995**, *34*, 4484–4489.
[36] U. S. Schubert, H. Hofmeier, G. R. Newkome, *Modern Terpyridine Chemistry*, Wiley-VCH, Weinheim, **2006**, pp. 37–68.
[37] W. Zhang, C. Bensimon, R. J. Crutchley, *Inorg. Chem.* **1993**, *32*, 5808–5812.
[38] D. Chatterjee, *J. Chem. Sci.* **1999**, *111*, 437–442.
[39] R. A. Reinhardt, J. S. Coe, *Inorg. Chim. Acta* **1969**, *3*, 438–440.
[40] B. K. Chan, M. A. Ciufolini, *J. Org. Chem.* **2007**, *72*, 8489–8495.
[41] V. Gabelica, F. Rosu, M. Witt, G. Baykut, E. De Pauw, *Rapid Commun. Mass Spectrom.* **2005**, *19*, 201–208.

Received: July 26, 2011
Published online: October 18, 2011

 © 2011 Wiley-VCH Verlag GmbH & Co. KGaA, Weinheim